

# High temporal and spatial resolution cine MRI for characterizing valvular and cardiac alterations in a genetic mouse model of valve disease

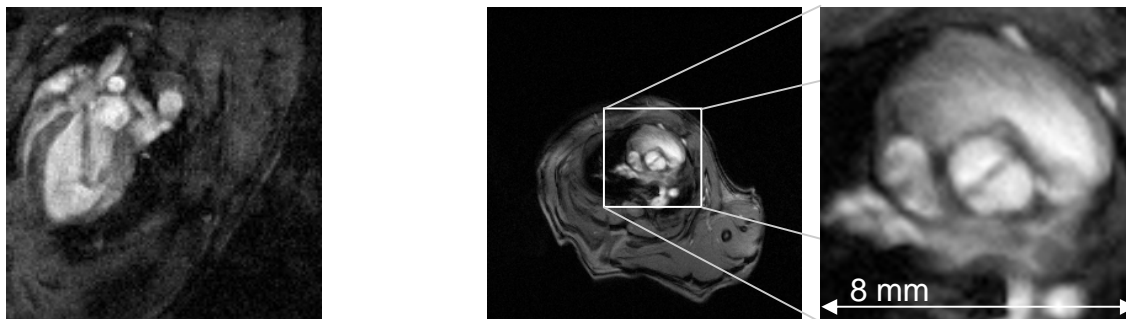
F. Kober<sup>1</sup>, S. Zaffran<sup>2</sup>, P. Topilko<sup>3</sup>, P. J. Cozzone<sup>1</sup>, and M. Bernard<sup>1</sup>

<sup>1</sup>Centre de Résonance Magnétique Biologique et Médicale (CRMBM), UMR CNRS N°6612, Faculté de Médecine, Université de la Méditerranée, Marseille, France, <sup>2</sup>Institut de Biologie du Développement de Marseille-Luminy, CNRS UMR N°6216, Marseille, France, <sup>3</sup>Biologie Moléculaire du Développement, Inserm U784, ENS, Paris, France

**Background and objectives:** Aortic and mitral valvular heart disease are responsible for heart failure and a contributing factor in heart stroke. In many cases, adult valvular lesions appear similar to the embryonic proliferative expansion phase, since they exhibit accumulation of EC matrix and myofibroblasts. Thus, lessons learned from valvulogenesis may provide insight into the molecular basis of adult valvular disease. An earlier analysis showed that absence of the transcriptional factor *Krox20* (also named EGR2 (1)) leads to valve defects. The objective of the present study was to assess the consequences of these valve defects on left-ventricular (LV) function and morphology *in vivo* using high-resolution MRI.

**Methods:** Since homozygous *Krox20* mice die shortly after birth, only 10-month-old heterozygous mice (n=10) were included in this study. A group of age-matched control mice (n=4) was assessed for comparison. The mice were anesthetized using isoflurane and inserted in a 20mm birdcage resonator. They underwent the following MRI protocol on a vertical Bruker Avance 500 WB system at 11.75T: After positioning and standard adjustments, a gradient-echo bright blood cine MRI sequence without flow compensation was used to obtain mid-ventricular short-axis and 4-chamber long-axis series of the heart. The sequence type and the parameters were chosen such as to obtain high spatial and temporal resolution with precise timing (TR/TE=5.1/1.2ms, 25 phases, FOV=30mm, matrix 256x256, cardiac and respiratory gating). An additional series was obtained in a plane perpendicular to the aortic root at the aortic valve level. An ellipsoid model was used to determine major parameters of LV function and morphology. Images in mid-systole were used to evaluate valvular morphology. Valvular function was assessed indirectly by qualifying left ventricular flow patterns on the 4-chamber long-axis views.

**Results:** Five of the heterozygous mice had heart defects while none of the controls showed abnormalities. Signal voids in LV



chamber blood allowed the observation of one severe regurgitation (left figure) by signal voids induced by rapidly flowing blood. Direct observation of a valvular malformation was possible in one case of bicuspid aortic valve (right figure), whereas all other animals had tricuspid valves. Severe left ventricular hypertrophy and LVEF < 30% was observed in two cases, one of which also showed severe aortic regurgitation (right figure). Two other *krox20* animals (images not shown) showed subtle aortic regurgitations only during the initial LV filling phase, but without measurable impact on LV function at the time of the MR assessment.

**Conclusion:** MRI allowed morphologic characterization of valvular heart disease and the simultaneous detection of associated alterations of cardiac physiology in genetically modified living mice. High spatial resolution was necessary to identify valvular malformation and valvular function. The rapid motion of the valve leaflets on the one hand and the short duration of the regurgitation jet made the use of a very short repetition time a requirement. The study of this particular mouse model can give deeper insight into the cause of potential valvular malformations and their molecular background in humans.

## References:

(1) Schneider-Maunoury S. et al., (1993). Disruption of *Krox-20* Results in Alteration of Rhombomeres 3 and 5 in the Developing Hindbrain. *Cell*. Vol 75, 1199-1214.